$YBa_2Cu_3O_x/CeO_2/NdGaO_3$ epitaxial heterostructures at different substrate orientations.

I K Bdikin[#], I M Kotelyanskii, E K Raksha, A D Mashtakov, P B Mozhaev, P V Komissinskii and G A Ovsyannikov

Institute of Radio Engineering and Electronics RAS, 103907 Moscow, Russia,
[#] Institute of Solid State Physics, Chernogolovka, 142432, Moscow district, Russia.

ABSTRACT: $YBa_2Cu_3O_x/CeO_2$ epitaxial heterostructures were grown on $NdGaO_3$ substrates with surface orientation tilted from the (110) plane. Two types of epitaxial relations were observed for CeO_2 buffer layer, depending on deposition technique and deviation angle of the substrate surface from the (110) $NdGaO_3$ plane. The $YBa_2Cu_3O_x$ thin films on the CeO_2 buffer layer grow either oriented with c axis normal to substrate plane, or following the orientation of the <100> axes of the buffer layer. Observed changes in epitaxy can be explained with different film formation mechanisms at different deposition rates.

1. INTRODUCTION

Materials with perovskite structure are often used as substrates for $YBa_2Cu_3O_x$ (YBCO) thin film preparation due to their similarity with high-temperature superconductor structure and element composition. Utilization of buffer layers often is necessary to prevent chemical interaction between film and substrate or to provide better lattice match. Cerium oxide CeO_2 is one of the most often applied buffer layer materials, providing excellent lattice match and suppressing chemical interaction at temperatures up to 750 °C (Mashtakov 1997). Fluorite structure of CeO_2 differs substantially from the substrate and film perovskite structure, that can lead to changes in epitaxy of both buffer layer on the substrate and YBCO film on the buffer layer (Kotelyanskii 1996, Mozhaev 1999). Such changes can increase when substrate surface deviates from the standard crystallographic orientations.

In the present paper we study epitaxial relations of the CeO_2 films on $NdGaO_3$ (NGO) substrates with deviation of orientation form the standard crystallographic planes and growth of YBCO films on the obtained CeO_2/NGO heterostructures.

2. EXPERIMENTAL

(110), (120), (130) and (010) crystallographic orientations of NGO substrates were chosen for buffer layer deposition. This set of orientations is obtained as a result of substrate plane rotation around [001] NGO axis.

CeO_2 films with typical thickness 300-400 Å were deposited by RF-magnetron sputtering and by e-beam evaporation. RF-sputtering of Ce target was performed in $Ar/O_2 = 2/1$ atmosphere at pressure 1.4×10^{-2} mbar and $U_{dc} = 200$ V. Typical deposition rate was 50-70 Å/min. E-beam evapoiration of CeO_2 was performed at pressure $\leq 10^{-4}$ mbar with typical deposition rate 5 Å/min. Substrate temperature during deposition was held at 650-750 °C (Mashtakov 1997).

YBCO films with thickness about 1500 Å were deposited on the buffer layer surface using either DC-sputtering at high oxygen pressure or laser ablation techniques. Typical sputtering parameters were: pure oxygen pressure 4 mbar, discharge voltage 280 V, discharge current density on target 1.5-1.75 A/cm^2. Deposition rate was about 5 Å/min. Laser ablation was performed at

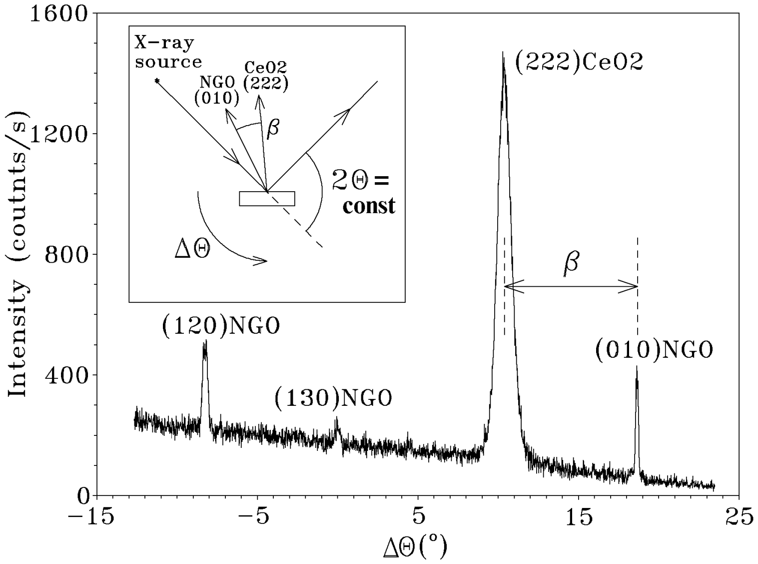

Fig. 1. Rocking curve in a wide angular scanning diapason. On the inset: schematics of the methodics. The angle between reflections is equal to the angle between normals to the crystallographic planes.

0.8 mbar O_2 and laser beam energy density of 1.7 J/cm^2; typical deposition rate was 400 Å/min. Deposition temperature in both cases was 750-780 °C. After deposition the YBCO films were oxygenated for 2 hours in 1 bar of O_2 at 350-450 °C (Mashtakov 1997, Mozhaev 1999).

Crystallographic properties of the obtained heterostructures were studied by X-ray diffractional techniques. For precise evaluation of the angles between crystallographic planes of the layers in the heterostructures the original methodics of rocking curve measurement in a wide angular scanning range was implemented. This methodics is illustrated on Fig. 1 with a sample of the rocking curve and geometry of the measurement on the inset. The 2θ-angle was set constant so, that the characteristic line of the X-ray source provided reflection peak from one of the substrate planes. The sample rotation around the (001) axis resulted in additional peaks on the rocking curve, corresponding to strong reflections from the film and substrate, due to wide-band X-ray radiation spectra. This technique allows direct and high precision measurement of the angles between film and substrate planes (for example β on Fig.1).

3. RESULTS

Two types of epitaxy were observed in CeO_2/NGO heterostructures, each of two variants (Fig. 2 and Table). “Standard” epitaxial relations of CeO_2 thin film on a (110) NGO substrate can be written as $(001)_C \| (110)_N$, $[110]_C \| [001]_N$ (Fig. 2, epitaxial type Ia); index ‘C’ denotes plane or direction in CeO_2 buffer layer, ‘Y’ – in the YBCO thin film and ‘N’ – in the NGO substrate. For all

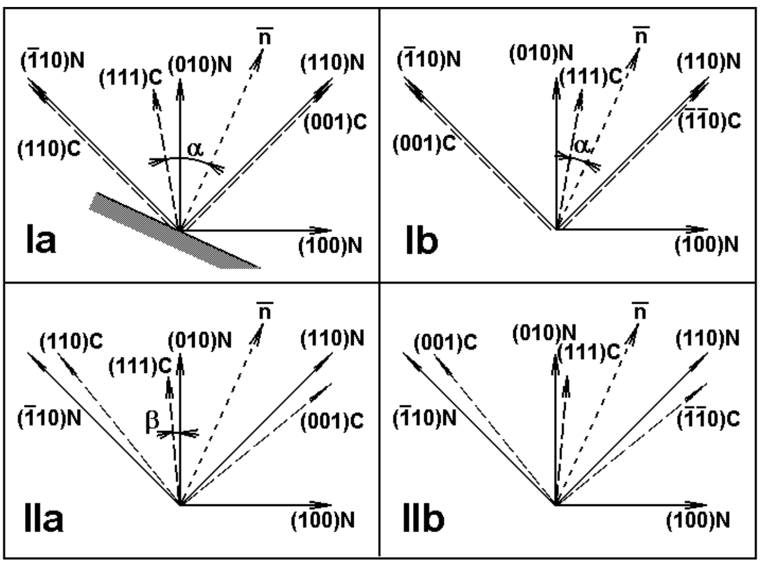

Fig. 2. Scematics of epitaxial growth of CeO_2 on the $NdGaO_3$ substrate with normal n. Variants a, b of the epitaxy types result from alignment of the [001] axis of CeO_2 along symmetrically equivalent directions [110] and [1̲10] of the substrate.

Table. Epitaxial type of CeO_2 growth on $NdGaO_3$ substrate at different deposition techniques and inclination of the [111] CeO_2 axis to substrate normal α and [010] $NdGaO_3$ axis β, correspondingly.

Substrate orientation	Deposition technique	Type of epitaxy	α, degree	β, degree
(110)	RF-sputtering	Ia	55	10
	e-beam evaporation	Ia	55	10
(120)	RF-sputtering	IIa	30	3
	e-beam evaporation	Ia	36	10
(130)	RF-sputtering	Ib	10	-8
		IIb (+IIa)	16 (and 22)	-3 (and 3)
	e-beam evaporation	Ia	28	10
(010)	e-beam evaporation	II	0	0

examined substrates the $[110]_C \| [001]_N$ relation remained correct, but CeO_2 orientation in the $(001)_N$ plane depended both on substrate surface orientation and on deposition technique. "Standard" epitaxy was observed for e-beam evaporated CeO_2 films on the (110), (120) and (130)-oriented substrates.

When RF-sputtering technique was used, "standard" epitaxy was observed only for (110) orientation of the substrate. For some of (130) substrates the same epitaxial type was observed (Fig. 2, Ib), but the $[001]_C$ was rotated 90°: $(001)_C \| (1\underline{1}0)_N$. RF-sputtered CeO_2 films mainly showed another type of epitaxy, when the $(111)_C$ plane is close to $(010)_N$ plane (Fig. 2, IIa and IIb). Similar to type I a and b variants of epitaxy, type II show two possible orientations of the $[001]_C$ axis: close to $[110]_N$ direction (IIa, (120) substrates) and close to $[\underline{1}10]_N$ direction (IIb, (130) substrates). Both IIa and IIb variants co-existed on one of (130) NGO substrates (see table). This type of epitaxy was observed only on the (010) substrates when e-beam evaporation technique was utilized.

The YBCO thin film orientation on the CeO_2 buffer layer depended mainly on the deposition technique. Laser ablation resulted in YBCO films oriented with the c axis normal to the substrate plane independent of buffer layer orientation. On Fig. 3, curve b, clear c-oriented film reflections can be seen on a $\theta/2\theta$-scan along the substrate normal. No YBCO alignment along the $[001]_C$ direction, inclined 31° from the substrate normal, is observed (Fig. 3, curve d). The X-ray diffractional φ-scans proved that the $\langle 100\rangle_Y$ axes are oriented along and perpendicular to the $[001]_N$ direction of the substrate.

DC sputtering at high oxygen pressure resulted in YBCO films oriented with the c axis along the $\langle 100\rangle_C$ directions of the buffer layer (Fig. 3, curves a and c). Cubic symmetry of CeO_2 results in 3 possible domain orientations of the YBCO film. Experimentally preferential domain formation was observed with axis c close to substrate normal, resulting in monodomain growth for Ia CeO_2 epitaxial

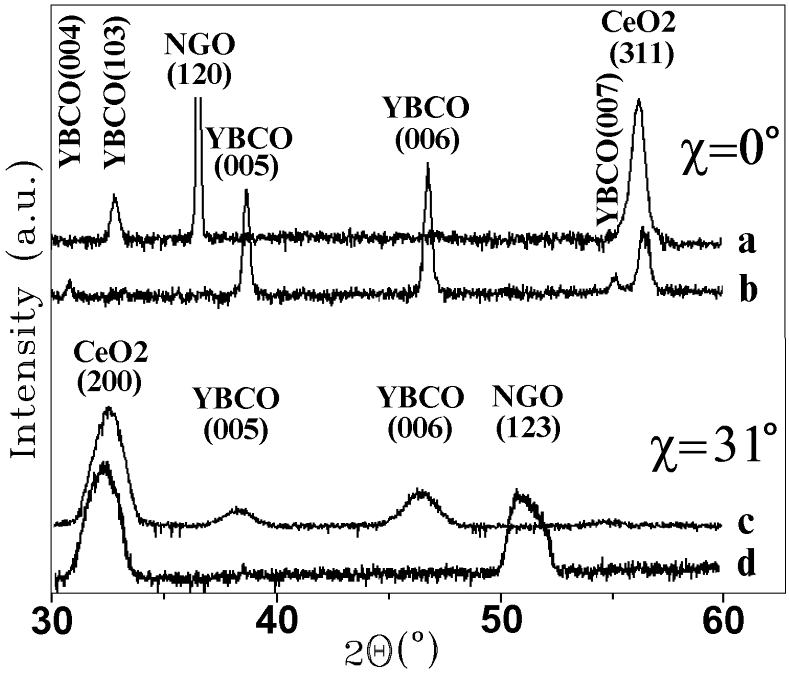

Fig. 3. X-ray diffractional $\theta/2\theta$-scans of the $YBCO/CeO_2$ heterostructures on the (120) $NdGaO_3$ substrates. Curves a, b represent scans along the substrate normal, while c and d curves show scans along the [001] CeO_2 direction, tilted 31 degrees from the substrate normal. Scans a, c were obtained from a sample with DC-sputtered YBCO film; scans b and d from a sample with YBCO film produced using laser ablation technique.

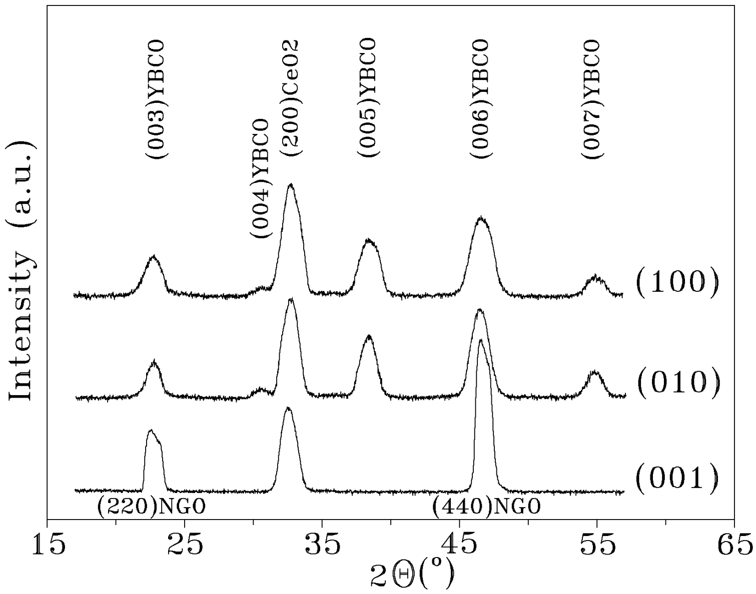

Fig. 4. X-ray diffractional θ/2θ-scans of the YBCO/CeO_2 heterostructure on a (130) $NdGaO_3$ substrate, deposited using DC-sputtering technique, along the <100> directions of the buffer layer. Only two YBCO domains are present at <100> CeO_2 orientations that are close to the substrate normal.

variants and two domains in Ib, IIb cases. On Fig. 4 the two-domain structure of the YBCO film on the (130) NGO substrate is revealed by θ/2θ-scans along the $<100>_C$ directions of the buffer layer. Three YBCO domains were observed in case IIa, when all CeO_2 <100> directions are almost uniformly inclined from the (120) substrate normal.

4. DISCUSSION

The epitaxial relations in the YBCO/CeO_2/NGO heterostructures depend strongly on deposition technique and deviation from crystallographic planes. Rotation of the substrate plane from $(110)_N$ to $(010)_N$ crystallographic planes of NGO results in change of epitaxy from type I to type II. Utilization of RF-sputtering technique results in change of the type of epitaxy even at deviation angles of 18° ((120) NGO substrate), while when e-beam evaporation is used, epitaxy type changes at deviation angles more than 26°. Difference in deposition rates can be possible reason of this distinction. Structure of the film, grown at low deposition rate, stronger depends on substrate atomic structure, while orientation of the film, grown at high deposition rate, depends on the opening facets surface energy. The $(111)_C$ facets provide minimal surface energy, favoring rotation of the $<111>_C$ axis towards substrate normal (Kotelyanskii 1996). Change from type I epitaxy to type II results in such rotation of $[111]_C$ axis, and happens at smaller deviation angle for high deposition rate RF-sputtering, than for low deposition rate e-beam evaporation. Similar reasons can lead to change from variant Ia to Ib epitaxy: the $[111]_C$ axis turns closer to normal.

YBCO thin film deposition on the CeO_2 buffer layer shows similar behavior. High deposition rate during laser ablation results in films with facets of minimal surface energy, i.e. $(001)_Y$-oriented films. At low deposition rate superconductor structure follows structure of the CeO_2 buffer layer. Formation of one or two domains instead of three confirms tendency of the film to grow with the c axis as close to substrate normal, as possible.

Authors would like to thank V.A. Lusanov, Yu.A. Boikov for fruitful discussion. The work was supported in part by the Russian Foundation for Basic Research, State Program of Russia "Modern Problems of the Solid State Physics", division "Superconductivity", Swedish Material Consortium and the INTAS program of the EU.

REFERENCES

Kotelyanskii I M et al 1996 Thin Solid Films **280**, 163
Mashtakov A D et al 1997 Inst Phys. Ser No158 (EUCAS'97), p.158
Mozhaev P B et al 1999 Technical Physics **44**, 242